Effect of Cation/Anion Structure on Phase Transition Behavior of Thermoresponsive Poly(IL) Gels for Solar Driven Water Purification

Takumi Takahashi[1], Masaki Tanaka[1], Takahiro Ichikawa[1], and Nobuhumi Nakamura*[1]

[1] Department of Biotechnology and Life Science, Tokyo University of Agriculture and Technology, Tokyo, Japan
nobu1@cc.tuat.ac.jp

Abstract. The increasing global population has led to a growing demand for clean water, accelerating the development of innovative, electricity-free purification systems for remote areas. A promising solution is a solar-driven water purification system that utilizes thermoresponsive hydrogels to adsorb and desorb water in response to temperature changes. This study investigates the influence of the molecular structures of both anions and cations in poly(IL) gels on their water adsorption/desorption behavior and phase transition temperature control. While previous research has focused on the properties of homopolymer gels, this study systematically investigated the distinct roles of the anionic and cationic structures by synthesizing and evaluating copolymer hydrogels with a unified anionic or cationic structure, respectively. We synthesized copolymer hydrogels with unified anionic and cationic structures, respectively, and evaluated their water adsorption/desorption capabilities. The results demonstrated that the hydrophilic/hydrophobic balance provided by the cationic structure is crucial for controlling the phase transition temperature while maintaining a dramatic water adsorption/desorption response to temperature changes. Specifically, in the system with varying anionic alkyl chain lengths, the LCST was shown to shift to lower temperatures as the chain length increased. Conversely, the system with varying cationic alkyl chain lengths exhibited linear dehydration behavior, suggesting that the [N4] cation structure plays a critical role as a scaffold enabling a cooperative phase transition. These findings contribute to the control of the phase transition behavior and the improvement of functions such as water adsorption/desorption capability in poly(IL) gels.

Keywords: Ionic liquid, hydrogel, LCST, purification

1 Introduction

In recent years, challenges related to water sustainability have become increasingly pressing due to factors such as population growth and climate change. Approximately 30% of the world's population currently lacks access to safe water resources, leading to a significant increase in demand for purified water [1–3] . Addressing these challenges necessitates the treatment and reuse of contaminated water, but conventional water treatment processes are highly energy-intensive, accounting for a substantial portion of global energy consumption [2]. Consequently, in regions with underdeveloped energy

S. C. Asih et al. (eds.), *Proceedings of the 19th International Conference on Quality in Research (QiR 2025)*, Advances in Engineering Research 303,
https://doi.org/10.2991/978-94-6239-717-0_13

infrastructure, securing energy sources for processes like desalination and wastewater treatment is difficult, severely hindering access to safe water [2].

To overcome these issues, solar-driven water purification systems have garnered significant attention. These systems typically comprise two main processes: solar vapor generation (SVG) and water vapor collection [4]. In SVG, porous photothermal materials are immersed in water and exposed to solar irradiation. The heat generated by these materials causes water to evaporate, allowing for purification at temperatures below its boiling point [4,5]. Numerous studies have explored various shapes and materials for SVG to enhance water evaporation efficiency [4–19].

However, a persistent challenge with these two-process systems (SVG and water vapor collection) has been reduced water recovery efficiency. This reduction stems from issues like steam mist obstructing solar light transmission and heat loss from the latent heat of vaporization [20]. To address this, a novel solar-driven water purification system was proposed [21]. This system enables the recovery of liquid water directly through solar irradiation without the need for evaporation, by utilizing materials that combine thermoresponsive hydrogels, photothermal materials, and adsorbents. The materials used in this system are fabricated by attaching black, pollutant-adsorbing polymeric materials such as polydopamine (PDA), MXene, carboxylic multi-walled carbon nanotubes, and carbon dots to the surface of poly-N-isopropylacrylamide (PNIPAM) gels, which exhibit lower critical solution temperature (LCST)-type phase transition behavior, swelling by absorbing water upon cooling and contracting by expelling water upon heating[20–26]. Furthermore, attaching sodium alginate or chitosan to this surface can enhance the pollutant adsorption capacity[21,23,25,26]. When the gel swells in contaminated water, pollutants can be adsorbed on the gel surface. Upon solar irradiation, the gel heats up and contracts while retaining the adsorbed pollutants, expelling purified water solely by solar irradiation (Figure 1).

While PNIPAM gels are commonly used as thermoresponsive hydrogels, they are obtained by polymerizing non-ionic monomers with low molecular designability, making their properties, especially the LCST, difficult to control. This limitation poses a challenge for their application in diverse temperature environments worldwide. To overcome this, we previously proposed the use of thermoresponsive ionic liquid (IL)-derived polyelectrolyte hydrogels (poly(IL) gels) as thermoresponsive hydrogels, leveraging the high molecular designability of ionic liquids [27]. Ionic liquids are low molecular weight salts composed of organic anions and cations, some of which have been reported to exhibit LCST-type phase transition behavior when mixed with water.[28–31] Similarly, poly(IL) gels, obtained by copolymerizing IL monomers with polymerizable groups and a cross-linker, have been reported to exhibit LCST-type phase transition behavior akin to PNIPAM gels [32–35]. We successfully developed a hydrogel with a controllable phase transition temperature based on the poly(IL) gel obtained by polymerizing the IL monomer N,N-dibutyl-N-(4-vinylbenzyl)butan-1-aminium 1-hexanesulfonate ([N4][C6]) (Figure 2) [27]. Furthermore, by functionalizing this hydrogel with PDA, a black polymer with pollutant adsorption capabilities, we successfully fabricated solar-driven water purification materials[27].

While previous research has led to the development of thermoresponsive poly(IL) gels with controllable phase transition temperatures and their application in solar-driven water purification, further elucidation of their detailed thermoresponsive properties and correlation with molecular structure is necessary[27]. However, previous studies have focused on homopolymer gels, and the individual roles of the cation and anion in enabling the cooperative phase transition have not been systematically investigated. Specifically, focusing on the molecular structures of ionic liquid monomers, which are key to thermoresponsiveness, previous studies reported that a homopolymer gel prepared using the IL monomer of [N4][C6] (the [N4][C6] gel) exhibits clear S-shaped phase transition behavior with rapid water expulsion upon small temperature changes[27]. In contrast, homopolymer gels prepared from each of the four IL monomers with different cationic alkyl chain lengths from [N4][C6] (N,N-dipropyl-N-(4-vinylbenzyl)propan-1-aminium 1-hexanesulfonate ([N3][C6]), N,N-dipentyl-N-(4-vinylbenzyl)pentan-1-aminium 1-hexanesulfonate ([N5][C6]) and different anionic alkyl chain lengths (N,N-dibutyl-N-(4-vinylbenzyl)butan-1-aminium 1-pentanesulfonate ([N4][C5]), N,N-dibutyl-N-(4-vinylbenzyl)butan-1-aminium 1-heptanesulfonate ([N4][C7]) showed no thermoresponsiveness (Figure 2) [27].

Therefore, this study aims to investigate in detail the influence of the molecular structures of anions and cations in poly(IL) gels on their water adsorption/desorption behavior and phase transition temperature control. Specifically, copolymer hydrogels with unified anionic or cationic structures were synthesized and their water adsorption/desorption capability and phase transition behavior were evaluated. These include poly([N3][C6]a-co-[N5][C6]1−a) gels and poly([N4][C5]$_a$-co-[N4][C7]$_{1-a}$) gels with 'a' values of 0.4, 0.5, and 0.6. As a result of evaluating the water adsorption/desorption capability, it was shown that the cationic structure is important for controlling the phase transition temperature while maintaining a dramatic water adsorption/desorption response to temperature changes. Particularly, a clear S-shaped phase transition was observed in the system where the anionic alkyl chain length was varied (poly([N4][C5]$_a$-co-[N4][C7]$_{1-a}$) gels with 'a' values of 0.4, 0.5, and 0.6), whereas a linear dehydration behavior was observed in the system where the cationic alkyl chain length was varied (poly([N3][C6]$_a$-co-[N5][C6]$_{1-a}$) gels with 'a' values of 0.4, 0.5, and 0.6). These findings provide important guidelines for controlling the phase transition behavior of poly(IL) gels at the molecular level and improving functions such as their water adsorption/desorption capability.

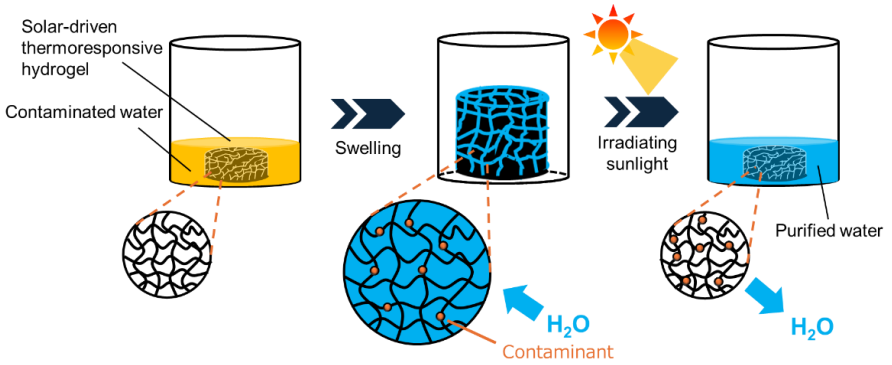

Figure 1 Schematic of the water purification mechanism using black polymer material and thermoresponsive hydrogel.

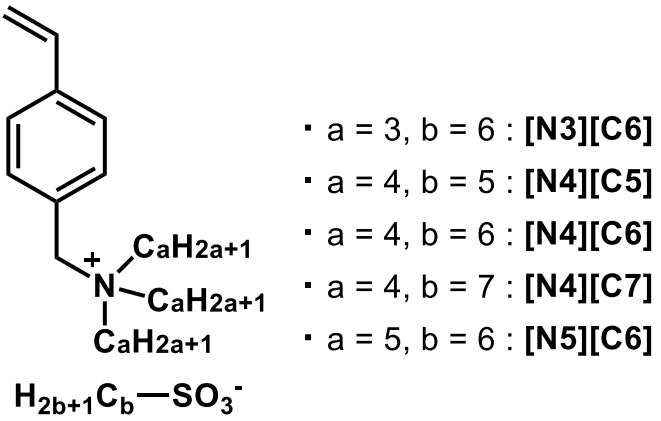

Figure 2 Structures of IL monomers.

2 Materials and Methods

2.1 Materials

Reagents were obtained from commercial suppliers and utilized without additional purification. Tripropylamine, tributylamine, triamylamine, sodium 1-pentanesulfonate (Na[C5]), sodium 1-hexanesulfonate (Na[C6]), sodium 1-heptanesulfonate (Na[C7]), 4-chloromethylstyrene, 2-hydroxy-4'-(2-hydroxyethoxy)-2-methylpropiophenone, and poly(ethylene glycol dimethacrylate) (average Mw=550) were procured from Tokyo Chemical Industry Co. Acetonitrile and dichloromethane were purchased from Kanto Chemical Industry Co., both with purities exceeding 99.5%. All specified purities for

the initial reagents were greater than 98.0%, with the exception of 4-chloromethylstyrene, which had a purity greater than 90.0%.

2.2 Synthesis of ammonium chloride precursors

The preparation method for these ammonium chlorides has been documented in prior literature, but for comprehensive understanding, a concise overview of the synthetic route is provided here[28]. In a reaction vial, 8.0 g (0.043 mol) of tributylamine was dissolved in 90 mL of acetonitrile. This solution was then incrementally added to 6.0 g (0.039 mol), equivalent to 0.9 molar equivalents, of 4-chloromethylstyrene. The quaternization reaction was conducted by heating the sealed vial in an oil bath at 40 °C for a duration of 72 hours. Post-reaction, the acetonitrile solvent was removed using a rotary evaporator. The resultant solid was subsequently washed with hexane. A final purification step involved suction filtration to isolate the white solid, followed by drying. This yielded the target N,N-dibutyl-N-(4-vinylbenzyl)butan-1-aminium chloride ([N4]Cl) with an 89% yield. Analogous procedures, substituting tributylamine with tripropylamine or triamylamine, led to the formation of N,N-dipropyl-N-(4-vinylbenzyl)propan-1-aminium chloride ([N3]Cl) (86% yield) and N,N-dipentyl-N-(4-vinylbenzyl)pentan-1-aminium chloride ([N5]Cl) (76% yield), respectively. The structural integrity of each synthesized ammonium chloride was verified via ^{1}H NMR spectroscopy (400 MHz, $CDCl_3$).

NMR Data:

- [N4]Cl 1H-NMR (400 MHz, CDCl3) δ = 7.44-7.54 (4H), 6.66-6.77 (1H), 5.78-5.87 (1H), 5.33-5.42 (1H), 4.95-4.99 (2H), 3.29-3.38 (6H), 1.74-1.83 (6H), 1.37-1.49 (6H), 0.97-1.05 (9H)
- [N3]Cl 1H-NMR (400 MHz, CDCl3) δ = 7.41-7.55 (4H), 6.62-6.78 (1H), 5.77-5.89 (1H), 5.33-5.42 (1H), 4.96-5.00 (2H), 3.22-3.32 (6H), 1.84-1.96 (6H), 0.97-1.08 (9H)
- [N5]Cl 1H-NMR (400 MHz, CDCl3) δ = 7.43-7.55 (4H), 6.65-6.79 (1H), 5.77-5.88 (1H), 5.34-5.43 (1H), 4.97-5.01 (2H), 3.28-3.40 (6H), 1.69-1.85 (6H), 1.29-1.46 (12H), 0.87-0.97 (9H)

2.3 Synthesis of the IL monomers via anion exchange

The synthesis of these ionic liquid monomers also follows established procedures [27], provided here for complete methodological clarity. IL monomers were synthesized through an anion exchange reaction involving [N3]Cl, [N4]Cl, or [N5]Cl with their respective alkali salts. As a representative example, the preparation of [N4] 1-pentanesulfonate ([N4][C5]) involved combining 7.74 g (0.02 mol) of [N4]Cl with 3.83 g (0.022 mol) of Na[C6] (1.1 molar equivalents) in 50 mL of deionized water. This mixture was continuously stirred at room temperature overnight. Subsequently, 200 mL of dichloro-

methane was introduced into the solution. The organic phase was then subjected to multiple washes with water until a silver nitrate test confirmed the absence of AgCl precipitate. Evaporation of the dichloromethane yielded [N4][C5] as a clear liquid. The structures of all prepared ILs were confirmed using ^{1}H NMR spectroscopy (400 MHz, $CDCl_3$).

NMR Data:

- [N4][C5] 1H-NMR (400 MHz, CDCl3) δ = 7.41-7.51 (4H), 6.67-6.77 (1H), 5.80-5.86 (1H), 5.35-5.40 (1H), 4.75-4.80 (2H), 3.21-3.30 (6H), 2.81-2.87 (2H), 1.73-1.91 (8H), 1.27-1.51 (10H), 0.99-1.04 (9H), 0.84-0.90 (3H) (76% yield)
- [N4][C7] 1H-NMR (400 MHz, CDCl3) δ = 7.40-7.51 (4H), 6.67-6.76 (1H), 5.79-5.86 (1H), 5.35-5.40 (1H), 4.74-4.79 (2H), 3.18-3.29 (6H), 2.80-2.87 (2H), 1.71-1.90 (8H), 1.22-1.49 (14H), 0.99-1.05 (9H), 0.81-0.89 (3H) (46% yield)
- [N3][C6] 1H-NMR (400 MHz, CDCl3) δ = 7.40-7.50 (4H), 6.67-6.76 (1H), 5.79-5.86 (1H), 5.35-5.40 (1H), 4.74-4.78 (2H), 3.16-3.25 (6H), 2.80-2.87 (2H), 1.79-1.94 (8H), 1.21-1.41 (6H), 0.99-1.07 (9H), 0.82-0.89 (3H) (58% yield)
- [N5][C6] 1H-NMR (400 MHz, CDCl3) δ = 7.41-7.50 (4H), 6.67-6.76 (1H), 5.79-5.87 (1H), 5.35-5.40 (1H), 4.77-4.81 (2H), 3.19-3.29 (6H), 2.80-2.87 (2H), 1.73-1.89 (8H), 1.24-1.45 (18H), 0.91-1.00 (9H), 0.81-0.88 (3H) (58% yield)

2.4 Preparation of poly(ionic liquid) gels

The synthesis protocol for these gels has been previously documented; nevertheless, for comprehensive procedural detail, a summary is outlined below[27]. Copolymer-type poly(IL) gels were fabricated using varying molar fractions of [N3][C6], [N4][C5], [N4][C7], and [N5][C6]. Specifically, poly([N4][C5]$_a$-co-[N4][C7]$_{1-a}$) gels and poly([N3][C6]$_a$-co-[N5][C6]$_{1-a}$) gels were prepared with '*a*' values of 0.4, 0.5, and 0.6. For each preparation, appropriate quantities of structurally distinct IL monomers were combined to achieve the desired copolymer composition. To this monomer mixture, poly(ethylene glycol dimethacrylate) (cross-linker) was added at 1 mol% relative to the total IL monomer content, and 2-hydroxy-4'-(2-hydroxyethoxy)-2-methylpropiophenone (radical initiator) was incorporated at 5 mol% relative to the total IL monomer. Subsequently, water was introduced at a concentration of 15 wt% based on the total monomer weight. Following sonication for degassing, the homogenous solution was carefully positioned between two quartz plates separated by a spacer. Polymerization was then initiated by irradiating the assembly with 365 nm light at an intensity of 2.3 $mWcm^{-2}$ for 1 hour at room temperature. The resulting IL gels underwent a minimum 48-hour soaking period in water to ensure the complete removal of any unreacted monomers.

2.5 Evaluation of the water content of the hydrogel

The water content of the synthesized IL gels was quantitatively determined using a gravimetric method. This involved measuring the mass of the fully water-saturated gel ($W_{water+polymer}$) and the mass of the completely dry gel ($W_{polymer}$), as defined by Equation (1).

$$(W_{water+polymer}-W_{polymer})/W_{polymer} \quad (1)$$

To obtain $W_{polymer}$, the hydrogel samples were subjected to vacuum degassing at an elevated temperature of 80 °C until all absorbed water was completely removed.

3 Results

3.1 Phase transition behavior of hydrogels obtained by copolymerizing IL monomers with different cationic alkyl chain lengths at various ratios

Figure 3 shows the change in water content at each temperature for hydrogels obtained by copolymerizing IL monomers with the same anionic alkyl chain length but different cationic alkyl chain lengths ([N3][C6] and [N5][C6]).The poly($[N3][C6]_{0.6}$-co-$[N5][C6]_{0.4}$) gel swelled, absorbing approximately 17 times its own weight in water at 2°C. This gel desorbed water with heating and contracted to a state containing approximately 2 times its own weight in water at 70°C.The poly($[N3][C6]_{0.5}$-co-$[N5][C6]_{0.5}$) gel absorbed approximately 10 times its own weight in water at 2°C. This gel desorbed water with heating and almost completely contracted at 40°C, reaching a state containing approximately 0.8 times its own weight in water. The poly($[N3][C6]_{0.4}$-co-$[N5][C6]_{0.6}$) gel absorbed approximately 9 times its own weight in water at 2°C. This gel desorbed water with heating and almost completely contracted at 30°C, reaching a state containing approximately 0.2 times its own weight in water.

3.2 Phase transition behavior of hydrogels obtained by copolymerizing IL monomers with different anionic alkyl chain lengths at various ratios

Figure 4 shows the change in water content at each temperature for hydrogels obtained by copolymerizing IL monomers with the same cationic alkyl chain length but different anionic alkyl chain lengths ([N4][C5] and [N4][C7]). All hydrogels swelled, absorbing approximately 18 times their own weight in water at 2°C, and desorbed water with increasing temperature. At 70°C, they were shown to contract to a state containing approximately 1 time their own weight in water. Since these temperature-dependent water content data showed typical S-shaped behavior, fitting was performed using the following Boltzmann function (Equation 2):

$$y=A_2+(A_1-A_2)/(1+\exp((x-x_0)/dx)) \quad (2)$$

Here, y is the water content, x is the temperature, A_1 and A_2 are the maximum water content at low temperatures and the minimum water content at high temperatures, respectively, x_0 is the center temperature of the phase transition (corresponding to LCST), and *dx* is a parameter indicating the steepness of the phase transition. The parameters obtained from the fitting are shown in Table 1. As shown in Figure 4, the experimental data were well reproduced by the Boltzmann function. From the fitting, the LCST of poly([N4][C5]$_{0.6}$-co-[N4][C7]$_{0.4}$) gel was calculated to be $x_0 = 43.8 \pm 1.3$°C, the LCST of poly([N4][C5]$_{0.5}$-co-[N4][C7]$_{0.5}$) gel was $x_0 = 36.6 \pm 0.6$°C, and the LCST of poly([N4][C5]$_{0.4}$-co-[N4][C7]$_{0.6}$) gel was $x_0 = 26.1 \pm 1.7$°C.

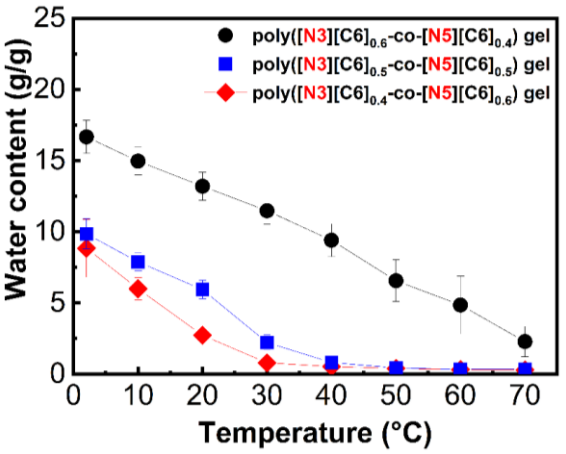

Figure 3 Temperature dependence of the water content of gels obtained by copolymerizing IL monomers with different cationic alkyl chain lengths at various ratios.

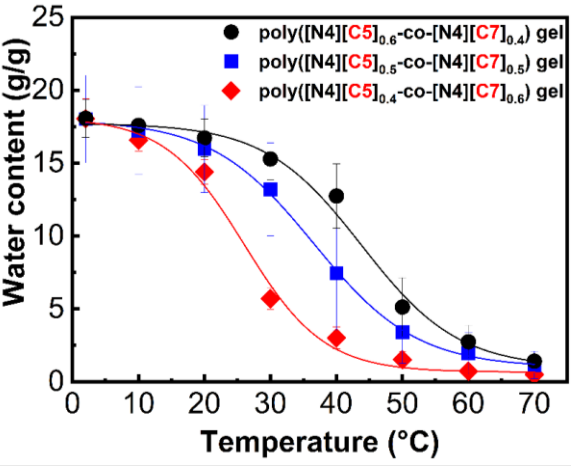

Figure 4 Temperature dependence of the water content of gels obtained by copolymerizing IL monomers with different anionic alkyl chain lengths at various ratios. The lines in the graph represent the Boltzmann fitting lines.

Table 1 Boltzmann fitting parameters for the temperature-dependent swelling curves of poly([N4][C5]-co-[N4][C7]) gels with different anionic alkyl chain lengths at various ratios

Parameter (Symbol)	poly([N4][C5]$_{0.6}$-co-[N4][C7]$_{0.4}$) gel	poly([N4][C5]$_{0.5}$-co-[N4][C7]$_{0.5}$) gel	poly([N4][C5]$_{0.4}$-co-[N4][C7]$_{0.6}$) gel	Unit	Description
Upper plateau (A_1)	17.7 ± 0.4	18.0 ± 0.3	18.1 ± 1.3	g/g	Water content at external low temperatures (fully swollen state)
Lower plateau (A_2)	1.0 ± 0.4	1.0 ± 0.1	0.7 ± 0.2	g/g	Water content at external high temperatures (fully deswollen state)
Transition temperature (x_0)	43.8 ± 1.3	36.6 ± 0.6	26.1 ± 1.7	°C	Center point of the sigmoid curve (corresponding to LCST)
Slope factor (dx)	7.3 ± 1.0	7.8 ± 0.5	6.0 ± 1.3	°C	Steepness of the transition curve (inverse related to cooperativity)
Adj. R-Square	0.997	0.9988	0.9876	-	Adjusted R-Square, accounts for number of predictors

4 Discussion

In this study, the influence of the alkyl chain length of IL monomers on the thermoresponsiveness of hydrogels, particularly their LCST-type phase transition behavior, was evaluated in detail. The obtained results show that these design parameters significantly affect the gel's swelling degree, the type of phase transition behavior, and the phase transition temperature.

4.1 Influence of alkyl chain length of cations on phase transition behavior

As shown in Figure 3, hydrogels obtained by copolymerizing IL monomers with the same anionic alkyl chain length but different cationic alkyl chain lengths ([N3][C6] and [N5][C6]) showed changes in water content temperature responsiveness depending on the composition ratio. Observing the initial swelling degree at 2 ℃, the poly([N3][C6]0.6-co-[N5][C6]0.4) gel absorbed approximately 17 times its own weight in water and swelled, the poly([N3][C6]0.5-co-[N5][C6]0.5) gel absorbed approximately 10 times its own weight in water, and the poly([N3][C6]0.4-co-[N5][C6]0.6) gel absorbed approximately 9 times its own weight in water, confirming a tendency for the initial swelling degree to decrease as the proportion of [N5][C6] increased. This is considered to be because the increase in the content of IL monomers containing [N5], which is a cation with a long alkyl chain, increases the hydrophobicity of the entire gel network, weakening the interaction with water in the low-temperature range.

Furthermore, a significant observation is that the decrease in water content in these hydrogels occurred linearly with increasing temperature. Unlike the sharp S-shaped phase transition exhibited by general LCST-type hydrogels, this linear behavior suggests that a clear cooperative phase transition was not induced in the gels copolymerized with [N3][C6] and [N5][C6]. This phenomenon suggests that the lack of a cooperative phase transition might stem from two main factors. First, the large difference in hydrophobicity between the [N3][C6] and [N5][C6] monomers could disrupt the formation of a homogeneous gel network. This inhomogeneity would prevent the synchronized expulsion of water molecules at a single, well-defined temperature. Second, the absence of the specific [N4] cation structure, which was shown in previous work to be critical for the sharp S-shaped transition, suggests that the balance of hydrophilic and hydrophobic interactions provided by this particular structure is essential for enabling the cooperative behavior.

4.2 Influence of alkyl chain length of anions on phase transition behavior

On the other hand, as shown in Figure 4, hydrogels obtained by copolymerizing IL monomers with the same cationic alkyl chain length but different anionic alkyl chain lengths ([N4][C5] and [N4][C7]) commonly showed an S-shaped temperature dependency of water content. This clearly confirms that these hydrogels exhibit distinct LCST-

type phase transition behavior. All gels showed a high swelling degree of approximately 18 times their own weight at 2°C and a similar swelling/deswelling behavior, contracting to approximately 1 time their own weight at 70°C, indicating that the basic thermoresponsive mechanism is maintained within these composition ranges.

As a result of fitting using the Boltzmann function to quantitatively evaluate this S-shaped behavior (Table 1), it became clear that the anionic alkyl chain length has a significant influence on the LCST. The LCST of poly([N4][C5]0.6-co-[N4][C7]0.4) gel was 43.8 ± 1.3 °C, the LCST of poly([N4][C5]0.5-co-[N4][C7]0.5) gel was 36.6 ± 0.6 °C, and the LCST of poly([N4][C5]0.4-co-[N4][C7]0.6) gel was 26.1 ± 1.7 °C. These results show that the LCST shifts to lower temperatures as the alkyl chain length of the anion in the IL monomer increases (i.e., as the content of [N4][C7] increases). This decrease in LCST can be interpreted as the introduction of IL monomers containing [C7], which is a long alkyl chain anion, increasing the overall hydrophobicity of the gel network. Hydrophobic interactions overcome the interaction with hydrated water as the temperature rises, serving as the driving force for gel contraction. As the anionic alkyl chain length becomes longer, these hydrophobic interactions become dominant at lower temperatures, causing the gel to start dehydration and contraction at a lower temperature. This is consistent with the general understanding that LCST is strongly dependent on the gel's hydrophobicity/hydrophilicity balance. Furthermore, comparing the dx parameter (indicating the steepness of the phase transition) in Table 1 provides insight into the cooperativity of the phase transition of these gels. For example, the poly([N4][C5]0.5-co-[N4][C7]0.5) gel showed a slightly larger value of dx=7.8±0.5 °C compared to the other two gels (with dx values of approximately 7.3 and 6.0). This may suggest that the phase transition tends to proceed somewhat more gradually in gels with an intermediate composition ratio Further investigation into network structural inhomogeneity and the complexity of these interactions is needed to provide a more definitive explanation for these subtle differences in steepness.

4.3 Overall influence of IL monomer structure on phase transition behavior

The results of this study clearly show that the alkyl chain lengths of both the cation and anion of IL monomers exert significant influences on the thermoresponsiveness of hydrogels. In our previous research, we reported that a homopolymer gel prepared using the IL monomer [N4][C6] (an IL monomer not explicitly dealt with in this study), specifically the [N4][C6] gel, exhibits clear S-shaped phase transition behavior, whereas homopolymer gels prepared from each of the four IL monomers investigated in this study ([N3][C6], [N4][C5], [N4][C7], [N5][C6]) showed no thermoresponsiveness[27]. Against this background, in the present study, the system in which the anion was unified to [C6] and the cationic alkyl chain length was varied (copolymers of [N3][C6] and [N5][C6]) showed no S-shaped phase transition, and a gradual dehydration behavior was observed. On the other hand, the system in which the cation was unified to [N4] and the anionic alkyl chain length was varied (copolymers of [N4][C5] and [N4][C7]) showed clear LCST-type phase transition. This difference is probably attributable to

the differences in the mode of hydrogen bonding and hydrophobic interactions that cations and anions form with water molecules within the gel network.

Particularly, considering the reported characteristics of the [N4][C6] gel in conjunction with the results of this study, it is strongly suggested that the structure of the [N4] cation plays a crucial role as a scaffold enabling a cooperative phase transition that responds dramatically to temperature changes. Furthermore, it is plausible that the [C6] anion contributes to optimizing this phase transition behavior.

These findings indicate that the molecular structural design of IL monomers is extremely important for designing responsive materials that function at specific temperatures.

5 Conclusion

In this study, we comprehensively investigated the influence of the molecular structures of both cations and anions in ionic liquid (IL) monomers on the water adsorption/desorption behavior and phase transition temperature control of thermoresponsive poly(IL) gels.

Hydrogels prepared by copolymerizing IL monomers with identical anionic alkyl chain lengths but varying cationic alkyl chain lengths ([N3][C6] and [N5][C6]) exhibited changes in water content temperature responsiveness based on their composition ratio and showed a linear dehydration behavior. This suggests that a clear cooperative phase transition was not induced, possibly due to factors such as a large difference in hydrophilicity/hydrophobicity between the two IL monomers.

Conversely, hydrogels prepared by copolymerizing IL monomers with identical cationic alkyl chain lengths but varying anionic alkyl chain lengths ([N4][C5] and [N4][C7]) exhibited clear S-shaped LCST-type phase transition behavior. In this system, it became evident that the LCST shifted to lower temperatures as the anionic alkyl chain length increased. This result indicates that the anion structure plays a crucial role in effectively adjusting the gel's hydrophobicity/hydrophilicity balance and controlling the phase transition temperature.

Considering the previously reported clear S-shaped phase transition behavior of the [N4][C6] homopolymer gel alongside the finding that the homopolymer gels prepared from [N3][C6], [N4][C5], [N4][C7], and [N5][C6] in this study showed no thermoresponsiveness, it is strongly suggested that the structure of the [N4] cation is important as a scaffold enabling a cooperative phase transition that responds dramatically to temperature changes. Furthermore, it is plausible that the [C6] anion contributes to optimizing this phase transition behavior.

These results provide crucial guidelines for precisely controlling the phase transition behavior of poly(IL) gels at the molecular level. It was particularly clarified that the molecular structural design of both cations and anions is extremely important for enhancing functions such as water adsorption/desorption capability in responsive materials that function at specific temperatures, especially for solar-driven water purification

systems. Future research is expected to further elucidate the correlation with microstructural changes in these mechanisms through additional physicochemical characterization techniques such as DSC and SAXS.

Acknowledgements

Include acknowledgments as appropriate. List individuals or institutions here that provided help and assistance during the research, such as offering grants, providing laboratory facilities, assisting with writing, or proofreading the article.

Nomenclature

poly(IL) gels ionic liquid-derived polyelectrolyte gels
SVG solar vapor generation
LCST lower critical solution temperature
PDA polydopamine
[N4][C6] N,N-dibutyl-N-(4-vinylbenzyl) butan-1-aminium 1-hexanesulfonate
[N3][C6] N,N-dipropyl-N-(4-vinylbenzyl) propan-1-aminium 1-hexanesulfonate
[N5][C6] N,N-dipentyl-N-(4-vinylbenzyl) pentan-1-aminium 1-hexanesulfonate
[N4][C5] N,N-dibutyl-N-(4-vinylbenzyl) butan-1-aminium 1-pentanesulfonate
[N4][C7] N,N-dibutyl-N-(4-vinylbenzyl) butan-1-aminium 1-heptanesulfonate

Author Contributions

Takumi Takahashi: Conceptualiation, Data curation, Formal analysis, Investigation, Methodology, Validation, Visualiation, Writing – original draft, Writing – review & editing. Masaki Tanaka: Project administration, Writing – review & editing. Takahiro Ichikawa: Project administration, Resources, Writing – review & editing., Nobuhumi Nakamura: Conceptualization, Funding acquisition, Project administration, Resources, Supervision, Writing – original draft, Writing – review & editing.

Conflict of Interests

The authors declare that they have no known competing financial interests or personal relationships that could have appeared to influence the work reported in this paper.

Funding

Funding was provided by a Grant-in-Aid for Challenging Research (Exploratory) (23K18538 to N.N.) from Japan Society for the Promotion of Science (JSPS).

Data Availability

Data will be made available on request.

References

[1] Abbaszadegan M, Alum A, Kitajima M, Fujioka T, Matsui Y, Sano D, et al. Water Reuse—Retrospective Study on Sustainable Future Prospects. Water (Switzerland) 2025;17. https://doi.org/10.3390/w17060789.
[2] Magni M, Jones ER, Bierkens MFP, van Vliet MTH. Global energy consumption of water treatment technologies. Water Res 2025;277. https://doi.org/10.1016/j.watres.2025.123245.
[3] Amparo-Salcedo M, Pérez-Gimeno A, Navarro-Pedreño J. Water Security Under Climate Change: Challenges and Solutions Across 43 Countries. Water (Switzerland) 2025;17. https://doi.org/10.3390/w17050633.
[4] Miao Y, Wang H, Hou X, Yu K, Yang X, Bian Z. Solar interfacial evaporation: From evaporation material design, condensing unit application to practical applications. Chemical Engineering Journal 2025;513. https://doi.org/10.1016/j.cej.2025.162792.
[5] Cui Y, Liang X, Wang Y, Wang J, Lohwacharin J, Lichtfouse E, et al. Advances in Hydrogel-Based Photothermal Interfacial Solar Steam Generation: Classifications, Mechanisms, and Applications. Adv Funct Mater 2025. https://doi.org/10.1002/adfm.202509130.
[6] Zhang P, Liu F, Liao Q, Yao H, Geng H, Cheng H, et al. A Microstructured Graphene/Poly(N -isopropylacrylamide) Membrane for Intelligent Solar Water Evaporation . Angewandte Chemie 2018;130:16581–5. https://doi.org/10.1002/ange.201810345.
[7] Wang Y, Li W, Yang S, Liu Z, Meng G, Wu J, et al. A Hydrogel Evaporator with Adjustable Internal Water Content Distribution for Seawater Desalination. Colloids Surf A Physicochem Eng Asp 2025:137555. https://doi.org/10.1016/j.colsurfa.2025.137555.
[8] Zhang J, Zhang X, Mai B, Fu N, Wang S, Shang B, et al. Mussel-inspired MXene-functionalized sponge for solar-driven water purification: Photothermal-driven crude oil absorption, solar steam generation, and photothermal sterilization. Chemical Engineering Journal 2025;514. https://doi.org/10.1016/j.cej.2025.163237.
[9] Lv J, Pan L, Zhu Y, Zhang X, Yang L, Wang X, et al. Thermo-responsive hydrogel evaporator via In-Situ chromogenic strategy for high-efficiency solar desalination

with robust salt resistance. Chemical Engineering Journal 2025;516. https://doi.org/10.1016/j.cej.2025.164026.
[10] Liu G, Zhang Y, Liu W, Ren P, Hou C, Xie X, et al. Plasmon-enhanced biomass-template porous carbon with strong photothermal effect for efficient solar-driven evaporation. J Environ Chem Eng 2025;13. https://doi.org/10.1016/j.jece.2025.117338.
[11] Guo Y, Zhou X, Zhao F, Bae J, Rosenberger B, Yu G. Synergistic Energy Nanoconfinement and Water Activation in Hydrogels for Efficient Solar Water Desalination. ACS Nano 2019;13:7913–9. https://doi.org/10.1021/acsnano.9b02301.
[12] Ong WL, Lu W, Zhang T, Ho GW. Integrated Functionality of Photothermal Hydrogels and Membranes in Solar Water, Chemical, Mechanical, and Electrical Domains. Adv Mater Technol 2024. https://doi.org/10.1002/admt.202401110.
[13] Naranjo D, Paulo-Mirasol S, Lanzalaco S, Armelin E, García-Torres J, Torras J. Thermosensitive Hydrogel PNIPAAm-Alg-PEDOT for Sustainable and Efficient Water Purification Powered by Solar Energy. Adv Sustain Syst 2024. https://doi.org/10.1002/adsu.202400234.
[14] Wang Y, Wu X, Shao B, Yang X, Owens G, Xu H. Boosting solar steam generation by structure enhanced energy management. Sci Bull (Beijing) 2020;65:1380–8. https://doi.org/10.1016/j.scib.2020.04.036.
[15] Mu P, Zhang Z, Bai W, He J, Sun H, Zhu Z, et al. Superwetting Monolithic Hollow-Carbon-Nanotubes Aerogels with Hierarchically Nanoporous Structure for Efficient Solar Steam Generation. Adv Energy Mater 2019;9. https://doi.org/10.1002/aenm.201802158.
[16] Zheng Z, Li H, Zhang X, Jiang H, Geng X, Li S, et al. High-absorption solar steam device comprising Au@Bi2MoO6-CDs: Extraordinary desalination and electricity generation. Nano Energy 2020;68. https://doi.org/10.1016/j.nanoen.2019.104298.
[17] Wu X, Robson ME, Phelps JL, Tan JS, Shao B, Owens G, et al. A flexible photothermal cotton-CuS nanocage-agarose aerogel towards portable solar steam generation. Nano Energy 2019;56:708–15. https://doi.org/10.1016/j.nanoen.2018.12.008.
[18] Huo B, Jiang D, Cao X, Liang H, Liu Z, Li C, et al. N-doped graphene /carbon hybrid aerogels for efficient solar steam generation. Carbon N Y 2019;142:13–9. https://doi.org/10.1016/j.carbon.2018.10.008.
[19] Jing X, Chen L, Li Y, Yin H, Chen J, Su M, et al. Synergistic Effect Between 0D CQDs and 2D MXene to Enhance the Photothermal Conversion of Hydrogel Evaporators for Efficient Solar Water Evaporation, Photothermal Sensing and Electricity Generation. Small 2024. https://doi.org/10.1002/smll.202405587.
[20] Long Y, Long Y, Zhou J, Wang M, Chen Y, Huang J, et al. Temperature-sensitive gel with adjustable lower critical solution temperature for solar-driven water collection. Mater Today Energy 2025;48. https://doi.org/10.1016/j.mtener.2025.101803.
[21] Xu X, Ozden S, Bizmark N, Arnold CB, Datta SS, Priestley RD. A Bioinspired Elastic Hydrogel for Solar-Driven Water Purification. Advanced Materials 2021;33. https://doi.org/10.1002/adma.202007833.
[22] Xu X, Guillomaitre N, Christie KSS, Bay RK, Bizmark N, Datta SS, et al. Quick-Release Antifouling Hydrogels for Solar-Driven Water Purification. ACS Cent Sci 2022. https://doi.org/10.1021/acscentsci.2c01245.

[23] Singh S, Jelinek R. Sunlight-Activated Phase Transformation in Carbon Dot-Hydrogel Facilitates Water Purification and Optical Switching. ACS Appl Polym Mater 2020;2:2810–8. https://doi.org/10.1021/acsapm.0c00358.
[24] Wang M, Sun Z, Zhou J, Chen Y, Mu X, Zhang Z, et al. Robust and Temperature-Sensitive Hydrogels for High-Efficiency Water Harvesting Under Low Solar Energy Radiation. Solar RRL 2023;7. https://doi.org/10.1002/solr.202300041.
[25] Zhao Z, Zhang Z, Zhu Z, Zou X, Zhao Y, Shi J, et al. Photothermal responsive hydrogel for adsorbing heavy metal ions in aqueous solution. Colloids Surf A Physicochem Eng Asp 2022;651. https://doi.org/10.1016/j.colsurfa.2022.129425.
[26] Mei J, Jin Y, Bai L, Shang X, Zeng W. A mimosa-inspired photothermal-responsive multifunctional hydrogel for passive solar-driven efficient water purification. J Mater Chem A Mater 2023;11:26063–74. https://doi.org/10.1039/d3ta05272a.
[27] Takahashi T, Yoshida T, Tanaka M, Ichikawa T, Ohno H, Nakamura N. Control of phase transition temperature of thermoresponsive poly(ionic liquid) gels and application to a water purification system using these gels with polydopamine. Sep Purif Technol 2024;337. https://doi.org/10.1016/j.seppur.2024.126433.
[28] Kohno Y, Ohno H. Temperature-responsive ionic liquid/water interfaces: Relation between hydrophilicity of ions and dynamic phase change. Physical Chemistry Chemical Physics 2012;14:5063–70. https://doi.org/10.1039/c2cp24026b.
[29] Kohno Y, Arai H, Saita S, Ohno H. Material design of ionic liquids to show temperature-sensitive lcst-type phase transition after mixing with water. Aust J Chem 2011;64:1560–7. https://doi.org/10.1071/CH11278.
[30] Fukaya Y, Sekikawa K, Murata K, Nakamura N, Ohno H. Miscibility and phase behavior of water-dicarboxylic acid type ionic liquid mixed systems. Chemical Communications 2007:3089–91. https://doi.org/10.1039/b704992g.
[31] Fukumoto K, Ohno H. LCST-type phase changes of a mixture of water and ionic liquids derived from amino acids. Angewandte Chemie - International Edition 2007;46:1852–5. https://doi.org/10.1002/anie.200604402.
[32] Kohno Y, Gin DL, Noble RD, Ohno H. A thermoresponsive poly(ionic liquid) membrane enables concentration of proteins from aqueous media. Chemical Communications 2016;52:7497–500. https://doi.org/10.1039/c6cc02703b.
[33] Deguchi Y, Nakamura N, Ohno H. Thermoresponsive ionic liquid/water mixtures for separation and purification technologies. Sep Purif Technol 2020;251. https://doi.org/10.1016/j.seppur.2020.117286.
[34] Deguchi Y, Kohno Y, Ohno H. Reversible water uptake/release by thermoresponsive polyelectrolyte hydrogels derived from ionic liquids. Chemical Communications 2015;51:9287–90. https://doi.org/10.1039/c5cc02189h.
[35] Okafuji A, Kohno Y, Nakamura N, Ohno H. Design of thermoresponsive poly(ionic liquid) gels containing proline units to catalyse aldol reaction in water. Polymer (Guildf) 2018;134:20–3. https://doi.org/10.1016/j.polymer.2017.11.047.